Springer
Berlin
Heidelberg
New York
Barcelona
Hong Kong
London
Milan
Paris
Singapore
Tokyo

Applied Computational Electromagnetics

State of the Art and Future Trends

Edited by

Nikolaos K. Uzunoglu
Konstantina S. Nikita
Dimitra I. Kaklamani

National Technical University of Athens
Department of Electrical and Computer Engineering
9, Iroon Polytechniou Str.
15780 Zografos, Athens, Greece

Springer

Published in cooperation with NATO Scientific Affairs Division

'roceedings of the NATO Advanced Study Institute on Applied
:omputational Electromagnetics: State of the Art and Future Trends,
ıeld at the Island of Samos, Greece, July 26–August 4, 1997

ıbrary of Congress Cataloging-in-Publication Data applied for

)ie Deutsche Bibliothek – CIP-Einheitsaufnahme

\pplied computational electromagnetics: state of the art and future
rends; [proceedings of the NATO Advanced Study Institute on Applied
:omputational Electromagnetics: State of the Art and Future Trends,
ıeld at the Island of Samos, Greece, July 26–August 4, 1997]/ed.
)y Nikolaos K. Uzunoglu... Publ. in cooperation with NATO Scientific
\ffairs Division. – Berlin; Heidelberg; New York; Barcelona; Hong
<ong; London; Milan; Paris; Singapore; Tokyo: Springer, 2000
(NATO ASI series: Ser. F, Computer and systems sciences; Vol. 171)
ISBN 3-540-65819-X

\CM Computing Classification (1998): C.0, C.1.m, D.1.2, D.2.4, F.3.1, I.2.2, J.2

ISBN 3-540-65819-X Springer-Verlag Berlin Heidelberg New York

Typesetting: Camera-ready by editors
Printing: Strauss Offsetdruck, Mörlenbach Binding: Schäffer, Grünstadt
Printed on acid-free paper

SPIN: 10648729 – 45/3142PS – 5 4 3 2 1 0

Preface

ΘΕΟΣ ΑΕΙ ΓΕΩΜΕΤΡΕΙ

Epigram of the Academy of Plato in Athens

Electromagnetism, the science of forces arising from Amber (ΗΛΕΚΤΡΟΝ) and the stone of Magnesia (ΜΑΓΝΗΣΙΑ), has been the foundation of major scientific breakthroughs, such as Quantum Mechanics and Theory of Relativity, as well as most leading edge technologies of the twentieth century.

The accuracy of electromagnetic fields computations for engineering purposes has been significantly improved during the last decades, due to the development of efficient computational techniques and the availability of high performance computing.

The present book is based on the contributions and discussions developed during the NATO Advanced Study Institute on *Applied Computational Electromagnetics: State of the Art and Future Trends*, which has taken place in Hellas, on the island of Samos, very close to the birthplace of Electromagnetism. The book covers the fundamental concepts, recent developments and advanced applications of Integral Equation and Method of Moments Techniques, Finite Element and Boundary Element Methods, Finite Difference Time Domain and Transmission Line Methods. Furthermore, topics related to Computational Electromagnetics, such as Inverse Scattering, Semi-Analytical Methods and Parallel Processing Techniques are included. The collective presentation of the principal computational electromagnetics techniques, developed to handle diverse challenging leading edge technology problems, is expected to be useful to researchers and postgraduate students working in various topics of electromagnetic technologies.

We would like to thank the NATO International Scientific Exchange Programme for supporting the publication of the present book, as well as the Institute of Communication and Computer Systems, Athens and the Eastern Aegean Research and Training Institute, Samos, for their support.

Athens, December 1999

Nikolaos K. Uzunoglu
Konstantina S. Nikita
Dimitra I. Kaklamani

Contents

Large-Domain MoM for CAD of Antennas and Scatterers

Branko D. Popović and Branislav M. Notaroš

Department of Electrical Engineering, University of Belgrade, P.O. Box 35-54, 11120 Belgrade, Yugoslavia

Abstract. Common MoM-based procedures are of subdomain type, requiring a large number of complex unknowns per wavelength cubed (on the order of 3000). This limits the application of the method to structures not exceeding few wavelengths cubed. A possibility to extend the MoM to larger structures are large-domain procedures. This chapter is aimed at describing such a procedure, to illustrate it on a number of examples, and to demonstrate its relative advantages and disadvantages with respect to subdomain procedures. The principal conclusion is that large-domain procedures can analyse considerably larger structures on the same computer in the same amount of time. However, the complete algorithm requires probably much more time than one of the subdomain type, and to obtain an efficient large-domain computer code a complicated programming is indispensable. Nevertheless, the authors believe that, due to its advantages once the code has been completed, the large-domain MoM might replace subdomain MoM in relatively near future.

Keywords. Large-domain approximation, method of moments, CAD, antennas and scatterers

1 Introduction

The moment-methods (MoM) [1] used today are principally of subdomain type (e.g., [2-4]). This restricts the application of the methods to electrically relatively small structures. In the most general (and critical) case of a 3D inhomogeneous dielectric scatterer, for which a volume representation of currents is indispensable, the scatterer practically cannot exceed few wavelengths in any direction. This is principally due to a large number of unknowns, and to an excessive cpu time needed for the solution of the resulting system of equations.

In subdomain methods, electrically small domains are adopted for the approximation of the scatterer geometry. In these small domains, the unknown current (or equivalent current) distribution is approximated at the most by one-, two- or three-dimensional linear (rooftop) functions. It requires a minimum of about ten complex unknowns per vector component per wavelength. For an

inhomogeneous dielectric cube scatterer three wavelengths on a side, this amounts to over 75,000 unknowns for a 3D problem.

Large domains with higher-order approximations for the generalized current distribution have been used with the MoM only rarely (e.g., [5, 6]). With large domains, a reasonable approximation is obtained with about five complex unknowns per wavelength per current component. For a 3D dielectric cubic scatterer three wavelengths on a side, this amounts to about 10,000 unknowns. So, by using large instead of small domains, with appropriate higher-order basis functions, we can push the applicability of the MoM-based methods to their extreme boundaries.

The chapter outlines a large-domain MoM method for the analysis and CAD of general antennas and scatterers, including metallic and dielectric parts. The method uses large trilinear hexahedrons for approximating inhomogeneous dielectric elements, bilinear quadrilaterals for approximating metallic surfaces and those of homogeneous dielectric bodies, and cylinders, frustums and narrow strips for approximating wires. The problem of critical junctions is also treated. Possible excitation mechanisms are discussed, and two useful new excitation mechanisms, the line-delta and surface-delta generator, introduced. The loadings include two analogous novel, very useful, types, the line-delta and surface-delta loading. The generalized current distribution in such elements is approximated by three-dimensional polynomials of relatively high degree (up to about ten).

Several large-domain computer codes for the analysis of electromagnetic structures have been developed by the principal author and his former Ph.D. students. The first of these was "WireZeus", a highly efficient large-domain code for the analysis and CAD of wire and related structures. It is based on generalized Hallén-type equations and polynomial approximation of current along segments, and is described in detail elsewhere [7]. The latest is the General ElectroMagnetic code ("GEM"), a new powerful code for the analysis and CAD of a wide variety of structures composed of wires, frustums, surfaces, and dielectric bodies [8]. Since the codes have already been validated in open literature [5-10], in this chapter only representative new examples are presented, with comparisons with other results in only few cases.

However, for all the examples data on the number of unknowns and on time needed to all the system matrix and to solve the system of equations using the Gaussian elimination procedure are provided, so that interested readers may compare these codes with other available codes. It is hoped that this will help the reader to understand the advantages of a carefully designed large-domain MoM method over subdomain MoM methods.

2 Definition of Large-Domain MoM

In any numerical solution of electromagnetic problems we always have two basic steps: (1) approximation (or modeling) of geometry of the actual system, and (2) approximation (or modeling) of current (or other unknown) in the approximate system.

The terms "subdomain", "large-domain" and "entire-domain" method of moments refer simultaneously to the level of approximation of geometry, and of current distribution. A subdomain method implies an approximation of geometry by a large number of electrically small cells (e.g., small cubes or tetrahetrons in a 3D problem), with low-order (at the most linear) approximation of current in them. A large-domain method is obtained if geometry is approximated by a small number of basic elements (e.g., parallelepipeds in a 3D problem), and the current in each of these elements by a single high-order approximating function (e.g., by a high-degree polynomial). An entire-domain method can be defined as a large-domain method in which the approximation of geometry is achieved with very few elements (e.g., a long dipole wire antenna in which the two arms are considered as two elements, and current is approximated by a high-order approximating function along each of them).

There is no clear boundary between large-domain and entire-domain concept. For any electrically large object, we need to subdivide it automatically into smaller (although still large) subdomains (we cannot approximate current distribution accurately in too large domains). The term "large-domain" appears to be more appropriate in both cases, and we shall use it in that sense.

3 Large-Domain Approximation of Geometry

Geometrical elements from which a 3D electromagnetic system is composed are principally of three forms: wire segments (possibly curved and impedance loaded), conducting surfaces (also possibly curved and impedance loaded), and (possibly lossy) dielectric bodies of arbitrary shape.

For the approximation of wires, it is usual to adopt straight-wire segments. A straight-wire segment is defined uniquely by its starting and end points, and its radius (if the segment is conical, the starting and end radii need to be specified instead). As shown in Fig. 1the points along the segment are easily described by a local coordinate, e.g. u,

$$\mathbf{r}(u) = \mathbf{r}_{start} + (\mathbf{r}_{end} - \mathbf{r}_{start})u, \qquad 0 \le u \le 1 \tag{1}$$

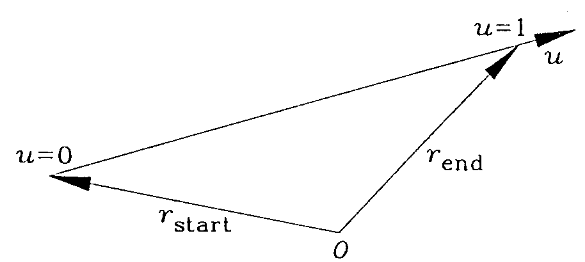

Fig. 1. Definition of straight-wire segment

In subdomain approach, conducting surfaces are usually approximated by a system of small triangles, or by small squares if surfaces are flat. This choice reflects the need that the surface elements can be simply and naturally interconnected. In large-domain approach, rectangles have been used, but they can be interconnected naturally only in certain cases. What is needed is a flexible surface element the sides of which, like in triangles, are defined uniquely by only two adjacent nodes, so that they can be interconnected naturally. In addition, it should be possible to define uniquely a local two-dimensional coordinate system for the description of points (and in the next step of the current distribution) over such an element.

An extension of the straight-wire segment concept in two dimensions leads to a space quadrilateral defined uniquely by its four vertices, i.e., having four parameters in its definition. The equation of such a quadrilateral is

$$\mathbf{r}(u,v) = \mathbf{r}_0 + \mathbf{r}_u u + \mathbf{r}_v v + \mathbf{r}_{uv} uv, \qquad 0 \le u, v \le 1 \tag{2}$$

Note that such a quadrilateral defines a unique, generally nonorthogonal $u-v$ coordinate system (Fig. 2). The coordinate lines in the system (note that the sides of the quadrilateral coincide with these lines) are straight [since, for v or u constant, eq. (2) becomes the same as eq. (1)]. Due to its bilinear expression, such a quadrilateral is termed a *bilinear quadrilateral*.

Bilinear quadrilaterals are very flexible, and can be used, with some approximations, to represent a wide variety of surfaces. Shown in Fig. 3 are two such cases. Fig. 3a shows the approximation of a triangle, and Fig. 3b the approximation of a complex body. Note that bilinear quadrilaterals cannot be concave or convex (this follows from the fact that the coordinate lines are straight), but only inflexed. This limits somewhat their application for accurate approximation of concave and convex surfaces.

Following the same reasoning, we wish to introduce a large hexahedral volume element limited by bilinear quadrilaterals as the element for the approximation of three-dimensional bodies. Such a *trilinear hexahedron* needs to be defined

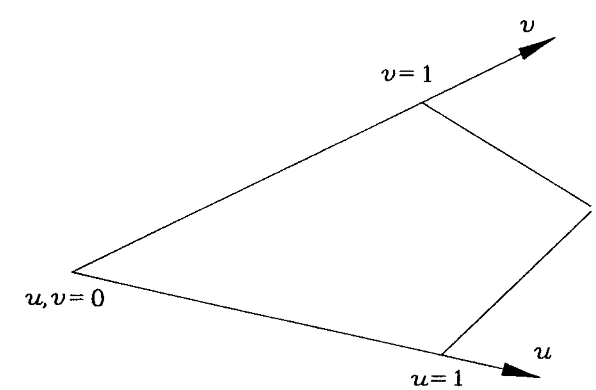

Fig. 2. A bilinear quadrilateral

uniquely by its eighth vertices. The equation of a point inside, or over, the hexahedron is given by

$$\mathbf{r}(u,v,w) = \mathbf{r}_0 + \mathbf{r}_u u + \mathbf{r}_v v + \mathbf{r}_w w + \mathbf{r}_{uv} uv + \mathbf{r}_{uw} uw + \mathbf{r}_{vw} vw + \mathbf{r}_{uvw} uvw, \quad 0 \le u, v, w \le 1 \tag{3}$$

and the hexahedron has the general form shown in Fig. 4. Note that the hexahedron edges coincide with the coordinate lines of a $(u-v-w)$ coordinate system, and its sides with the coordinate surfaces in such a system.

A variety of three-dimensional bodies can be approximated efficiently by a small number of such hexahedrons (Fig. 5). Fig. 5a shows the approximation of a circular cylinder, and Fig. 5b of a Gamma-shaped body. [Note that, for the formulation of boundary conditions for current density (or other unknown), adjacent hexahedrons must share the entire side, not only part of it].

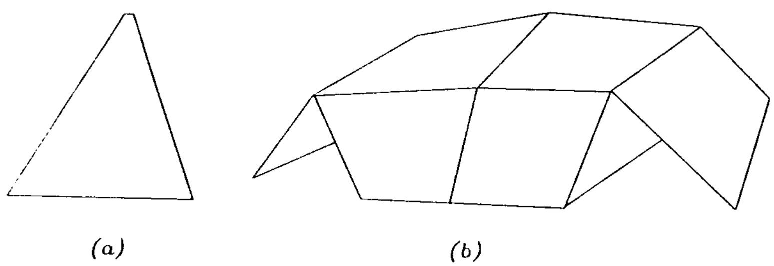

Fig. 3. Approximation of (a) a large triangle, and (b) a complex three- dimensional body by quadrilaterals

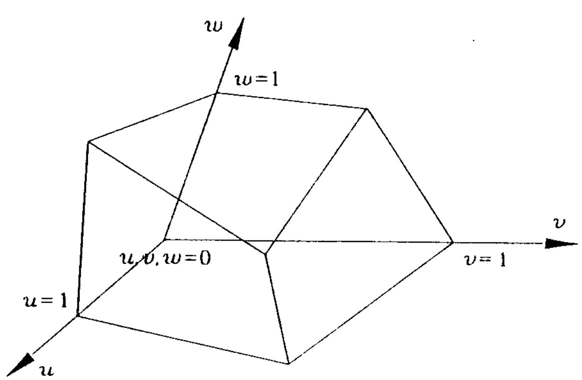

Fig. 4. A trilinear hexahedron and the local coordinate system

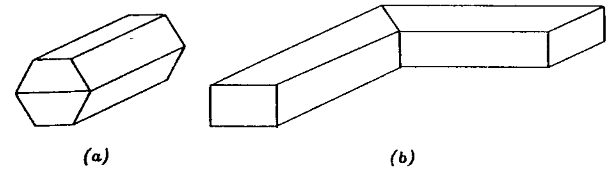

Fig. 5. Approximation by a small number of trilinear hexahedrons of (a) a circular cylinder, and (b) a Gamma-shaped body

4 Large-Domain Current Approximation

The geometrical elements for the approximation of 1D, 2D, and 3D bodies have natural (generally nonorthogonal) coordinate systems associated with them. By defining current density (or other unknown) in these elements so that its components are those in that local coordinate system, the analysis is greatly simplified. An additional simplification, which relates in particular to numerical evaluation of the integrals, is obtained if the basis functions are assumed to be powers in the local coordinates. Thus, we approximate current distribution along a wire segment by a polynomial [7]

$$I(u) = \sum_{i=0}^{n} I_i u^i \tag{4}$$

(see Fig. 1). We represent the u-component of the surface current over a bilinear quadrilateral as [9]

$$J_{su}(u,v) = \sum_{i=0}^{n_u} \sum_{j=0}^{n_v} J_{suij} u^i v^j \tag{5}$$

and in analogy the v-component (see Fig. 2). Finally, the u-component of the volume current inside a trilinear hexahedron is written in the form [11],

$$J_u(u,v,w) = \sum_{i=0}^{n_u} \sum_{j=0}^{n_v} \sum_{k=0}^{n_w} J_{uijk} u^i v^j w^k \tag{6}$$

and similarly for the other two components (see Fig. 4).

5 Boundary Conditions and Basis Functions

If we were able to solve the integral equations for current exactly, boundary conditions would be satisfied automatically. In an approximate solution, boundary conditions need always to be added to stabilize the solution. There is a variety of conditions that could be stipulated to hold across boundaries, but it appears that the following conditions stabilize the solution adequately:

a) The First Kirchhoff Law at all wire nodes (including free wire ends) [7].
b) Continuity of normal components of the surface-current density vector along the common side of two quadrilaterals [9]. This implies a zero normal component of surface-current density vector on a free side of a quadrilateral, since line charges do not exist along such a side.
c) The current-continuity equation for normal components of the volume current density vector over the common side of two adjacent hexahedrons and the surface charge density over that surface [10, 11].

To make the expressions for the boundary conditions as simple as possible, it is convenient to represent the current in all three cases as a sum of the following basis functions:

- two linear functions, of which one is zero at one, and the other at the other end of a wire, i.e., opposite side of a quadrilateral or hexahedron, and
- a corrective polynomial with zeros at the wire ends, i.e., at the opposite sides of a quadrilateral or hexahedron

6 Junctions of Elements

Junctions of elements deserve special attention, since their treatment may influence considerably the stability of the solution.

6.1 Junctions of the Same Type of Elements

The simplest junction is that of wires. If the wire radii do not differ significantly, the First Kirchhoff Law, as explained, suffices as the constraint for currents at the junction. (Note that in the point-matching solution the Second Kirchhoff Law, i.e., that all the segments meeting at a node have there the same scalar potential, was found to be very useful [7]).

In the case of a junction of several surfaces along a common side, the components of the surface-current density vectors along the side due to all the surfaces, at all the points along the side, must also satisfy the First Kirchhoff Law.

Physically, more than two hexahedrons cannot be interconnected over a common side, so that this case need not be considered.

6.2 Junctions of Different Types of Elements

The junction of a wire (or several wires meeting at the junction) and a surface can easily be approximated in the adopted model. The surface is divided into appropriate quadrilaterals about the junction, as in Fig. 6, and the First Kirchhoff Law is stipulated at the junction for the wires and the sides of the quadrilaterals adjacent to the junction [9].

Junctions of wires and bodies are rare and difficult to treat. A treatment similar to that for wires and surfaces is possible, but very complicated to implement.

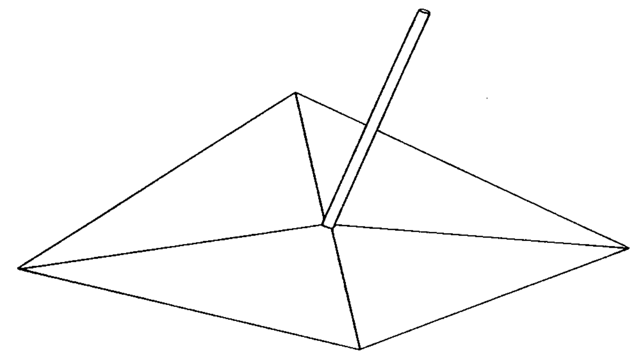

Fig. 6. Junctions of a wire and a surface, showing subdivision of the surface

Junctions of surfaces and bodies is allowed only if a quadrilateral surface coincides with a quadrilateral side of a hexahedron.

7 Generator and Load Models

The following generator and load models appear to be useful in the analysis of general structures:

- At wire-to-wire junctions: point-delta or magnetic TEM frill generator, and point-delta load. Note that for several wires meeting at a junction the TEM frill might lead to highly inaccurate, or even meaningless results.
- At wire-to-surface junctions: point-delta or magnetic TEM frill generator (with the same note as in the preceding case), and point-delta load.
- At surface-to-surface junctions: line-delta generator and load. This is a novel type of generator and load. It is assumed that across the common side of two quadrilaterals there is a nonzero voltage (ideal voltage generator, a generalization of the point-delta generator and load). In the case of a generator, this voltage equals the emf of the generator. In the case of a load, the voltage equals the product of the surface-current component normal to the common side and the specified transverse impedance of the common side.
- At volume-to-volume junctions: surface-delta generator and load. This is also a novel type of generator and load. It is assumed that there is a specified voltage across the common side of two hexahedrons. In the case of a generator, it is equal to the emf of the generator. In the case of a load, the voltage equals the product of the normal component of the current density vector and the transverse impedance of the common side of the two hexahedrons.

8 Equations and their Numerical Solution

The integral equations that can be used as the starting point in the large-domain analysis of electromagnetic structures are the same as in the subdomain analysis. We use the electric-field integral equation (EFIE),

$$\frac{\mathbf{J}}{\sigma_e} - \mathbf{E}(\mathbf{J}) = \mathbf{E}_{inc.} \quad (7)$$

and the two-potential integral equation (TPIE),

$$\frac{\mathbf{J}}{\sigma_e} + j\omega\mathbf{A}(\mathbf{J}) + \text{grad}[V(\mathbf{J})] = \mathbf{E}_{inc.} \quad (8)$$

In these equations, $\mathbf{J}$ is the unknown current density vector (line, surface or volume),

$$\mathbf{J} = \sigma_e \mathbf{E}_{total}, \qquad \sigma_e = \sigma + j\omega(\varepsilon - \varepsilon_0) \quad (9)$$

where $\mathbf{E}_{total}$ is the total electric field,

$$\mathbf{E}_{total} = \mathbf{E} + \mathbf{E}_{inc.} \quad (10)$$

In this equation, $\mathbf{E}$ is the electric field due to the currents,

$$\mathbf{E} = \mathbf{E}(\mathbf{J}) = \sum_{k=1}^{N_{el.}} \left[\mathbf{E}_k^{(u)} + \mathbf{E}_k^{(v)} + \mathbf{E}_k^{(w)}\right] \quad (11)$$

with $N_{el.}$ being the total number of elements in the geometrical model and $\mathbf{E}_{inc.}$ is the incident electric field which excites the structure.

A convenient unknown for volume scatterers is also the equivalent electric displacement vector [11-12],

$$\mathbf{D} = \varepsilon_e \mathbf{E}_{total} = \frac{\mathbf{J}}{j\omega}, \qquad \varepsilon_e = \varepsilon - j\frac{\sigma}{\omega}, \qquad K = \frac{\varepsilon_e - \varepsilon}{\varepsilon_e}, \quad (12)$$

where K is known as the electric constant of the scatterer.

The solution procedure of the integral equations may be any method-of-moment procedure. To obtain an independent check on the accuracy of the solution, four numerically independent large-domain numerical procedures were developed and mutually compared. These four procedures were [12]:

a) Point-matching solution of the EFIE, with $\mathbf{J}$ as unknown (PEJ method).
b) Point-matching solution of the EFIE, with $\mathbf{D}$ as unknown (PED method).
c) Galerkin solution of the TPIE, with $\mathbf{J}$ as unknown (GPJ method).
d) Galerkin solution of the TPIE, with $\mathbf{D}$ as unknown (GPD method).

Agreement of the results obtained by these four methods was found to be exceptionally good [12].

Finally, a note on the integration of the integrals is in order. In 3D case, the integrals are multiple quasi-singular integrals which require very large amount of computing time if integrated by brute force. Refined integration procedures are

therefore essential for an efficient and accurate solution of electromagnetic problems by large-domain approach. Basically, this requires the following:

- higher-order extractions of singularities, to enable large-domain integration by a low-order Gaussian quadrature formula,
- simultaneous integration of all integrals, to greatly reduce the number of operations, and
- elimination of redundant calculations

Evidently, these precautions require a lot of analytical derivations, and a careful and lengthy programming. However, once this is achieved, the evaluation of the system matrix requires less time than the solution of linear equations (by the Gaussian elimination method) with already 200-300 unknowns. Thus, for a large number of unknowns (few thousand), the principal part of the computing time becomes that for the solution of linear equations.

9 Results

All results presented below were obtained on an IBM PC Pentium 133 MHz. The pair of numbers of the form $T(t_1, t_2)$ give the matrix total time and matrix inversion time at the highest frequency considered (if more than one). $N = n$ shows the total number of unknowns, again for the highest frequency in the range.

9.1 A Biconical Antenna

A biconical antenna can be analyzed using the *GEM* code with great ease. We need only to specify the antenna as a wire antenna with different starting and fiend radii (one of which can be zero). Thus for the antenna sketched in Fig. 7 (which was optimized interactively for approximately lowest VSWR in the frequency range shown) we obtain the VSWR and the reflection coefficient versus frequency as in Fig. 8, with T (0.22, <0.01), and $N = 13$.

9.2 A Loop Antenna on Dielectric Core

A loop antenna on cubical dielectric core of relative permittivity $\varepsilon_r = 2.1$, conductivity $\sigma = 0$, side length $d = 5.08$ cm, and wire radius $a = 0.508$ cm, is analyzed next (Fig. 9). The core was considered as a single hexahedron, and the wire loop consisted of five straight segments.

The results for the antenna resistance and reactance are shown in Fig.10 (T(1.65,0.05), $N = 46$). Comparing these results with those in [13] (not shown in the figure), it is found that agreement is very good, although the latter subdomain method requires about $N = 3000$ unknowns, with the matrix inversion time about 7800 seconds.

9.3 CAD of a Waveguide Terminated in Pyramidal Horn

Consider now a section of a short-circuited waveguide excited by a coaxial probe, feeding a pyramidal horn, Fig. 11 (only one half of the symmetrical horn is snown). A General Radio horn of this type was considered, of the following dimensions: waveguide sides $a = 34.85$ mm, $b = 15.8$ mm; length of the waveguide $l = 41.1$ mm; horn sides $A = 160$ mm, $B = 122$ mm; horn length (from the end of the waveguide, along the system axis) $L = 120$ mm; monopole probe exciting the waveguide was a distance $d = 8$ mm from the waveguide shortcircuit, it was of height $h = 10.0$ mm, and of radius $r = 1.05$ mm. The horn was designed for a frequency of $f = 6$ GHz. Analysis with *GEM* [$T(1.04, < 0.01)$, $N = 20$]

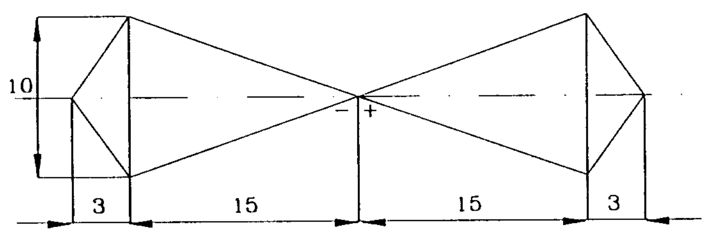

Fig. 7. Sketch of a biconical antenna. The dimensions are in cm

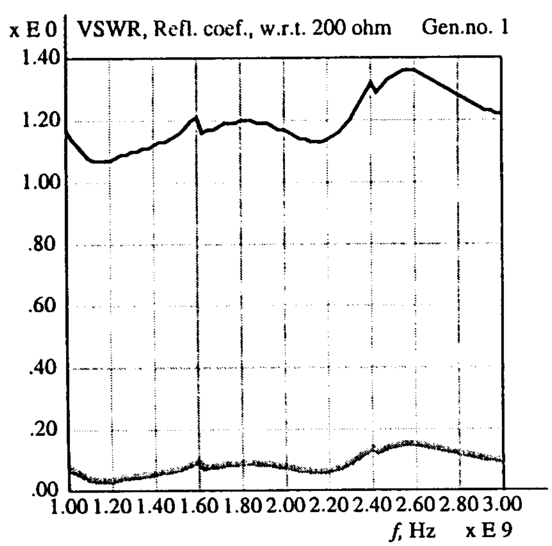

Fig. 8. VSWR for the biconical antenna in Fig.7 and described in the text

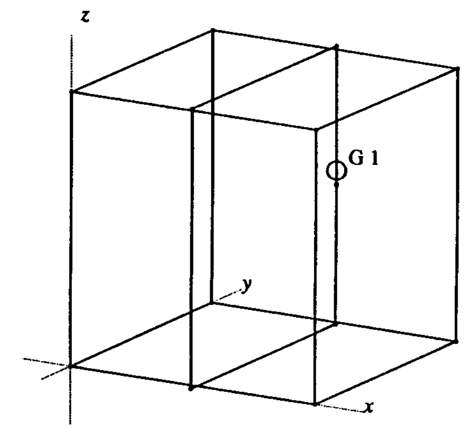

Fig. 9. A loop antenna on dielectric core. For details see text

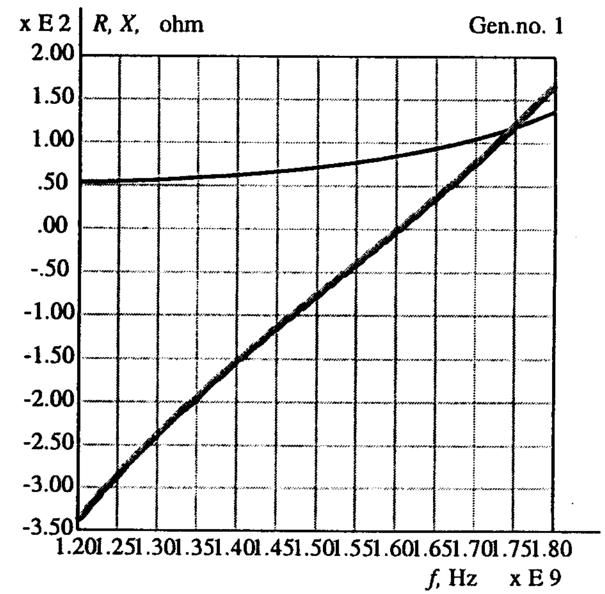

Fig. 10. *R* and *X* for the antenna in Fig. 9

resulted in the horn directivity of $D \approx 16.5$ dBI, and the monopole impedance of $Z_{input} = (50 - j1.6)\Omega$ ($VSWR = 1.03$), which differed from measured values for less than 3 per cent.

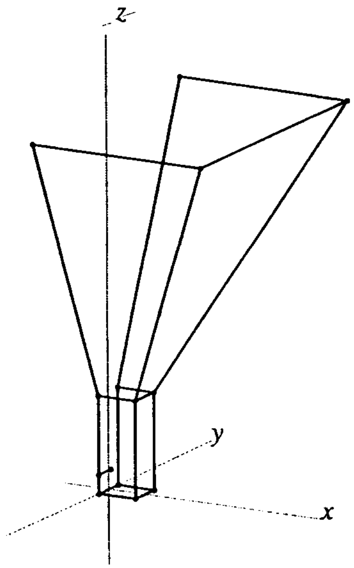

Fig. 11. Waveguide terminated in pyramidal horn (half of structure)

10 Conclusions

Large-domain moment methods have the following advantages over subdomain methods:

- For a 3D case, the number of unknowns is reduced by a factor of about 10, of matrix elements is reduced by a factor of about 100, and the matrix inversion time is reduced by a factor of about 1000.
- Consequently, analysis and CAD of much larger electromagnetic structures on the same computer by large-domain methods is possible than by subdomain methods.

Large-domain methods also have the following principal drawbacks with respect to subdomain methods:

- More complicated algorithm (including complicated algorithms for accurate and efficient integration of multiple integrals) and programming.

In spite of these drawbacks, it could be stated that large-domain MoM methods are much more efficient than subdomain methods. Nevertheless, large-domain methods at present are more a rarity than a rule.

Although any predictions are very uncertain, the authors anticipate the following likely future trends in the use of large-domain MoM methods:

- In 5-10 years, predominant use could be expected of large domains (higher order approximations) for solving EM problems.
- In 10-15 years, large domains (higher order approximations) will replace subdomains (i.e., low order approximations) in most applications.

References

[1] R. F. Harington, *Field Computation by Moment Methods*, New York, Macmillan, 1968.

[2] D. H. Schaubert, D. R. Wilton, and A. W. Glisson, "A tetrahedral modeling method for electromagnetic scattering by arbitrarily shaped inhomogeneous dielectric bodies," *IEEE Trans. Antennas Propagat.*, vol. 32, pp. 77-85, Jan. 1984.

[3] T. K. Sarkar, E. Arvas, and S. Ponnapalli, "Electromagnetic scattering from dielectric bodies," *IEEE Trans. Antennas Propagat.*, vol. 37, pp. 673-676, May 1989.

[4] P. Zwamborn and P. M. van der Berg, "The three-dimensional weak form of the conjugate gradient FFT method for solving scattering problems," *IEEE Trans. Microwave Theory Tech.*, vol. 40, pp. 1757-1766, Sep. 1992.

[5] B. D. Popović and B. M. Notaroš, "Entire-domain polynomial approximation of volume currents in the analysis of dielectric scatterers," *IEE Próc. Microw. Antennas Propagat.*, vol. 142, pp. 207-212, Mar. 1995.

[6] B. M. Notaroš and B. D. Popović, "Optimized entire-domain moment-method analysis of 3D dielectric scatterers," *Int. J. of Num. Modelling: Electr. Netw., Dev. and Fields*, vol. 10, pp. 177-192, Oct. 1997.

[7] B. D. Popović, *CAD of Wire Antennas and Related Radiating Structures*, Research Studies Press (John Wiley & Sons), New York - Chichester, 1991.

[8] B. M. Notaroš and B. D. Popović, *General electromagnetic code (GEM)*, Univ. of Belgrade, Yugoslavia, 1993-1998.

[9] B. D. Popović and B. M. Kolundžija, *Analysis of Metallic Antennas and Scatterers*, London, IEE, 1994.

[10] B. M. Notaroš and B. D. Popović, "General entire-domain method for analysis of dielectric scatterers," *IEE Proc. Microw. Antennas Propagat.*, vol. 143, pp. 498-504, Dec. 1996.

[11] B. M. Notaroš, *Numerical analysis of dielectric bodies of arbitrary shape and inhomogeneity in the electromagnetic field*, D. Sc. thesis, Dept. of EE, Univ. of Belgrade, Yugoslavia, 1995.

[12] B. D. Popović and B. M. Notaroš, "Moment-method analysis of volume dielectric scatterers. Four independent entire-domain solutions: is entire domain phylosophy a luxory or necessity in the method of moments?," *Int. J. of Microw. and Millimeter-Wave Comp.-Aided Eng.*, vol. 6, pp. 454- 473, 1996.

[13] J. P. Casey and R. Bansal, "Dielectrically loaded wire antennas," *IEE Proc., H*, vol. 135, pp. 103-110, April 1988.